

Unveiling Fragmentation of Plastic Particles during Biodegradation of Polystyrene and Polyethylene Foams in Mealworms: Highly Sensitive Detection and Digestive Modeling Prediction

Bo-Yu Peng, Shaoze Xiao, Ying Sun, Yurong Liu, Jiabin Chen, Xuefei Zhou, Wei-Min Wu,* and Yalei Zhang*



Cite This: *Environ. Sci. Technol.* 2023, 57, 15099–15111



Read Online

ACCESS |

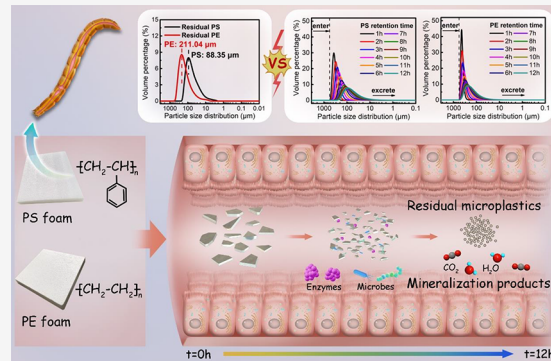
Metrics & More

Article Recommendations

Supporting Information

ABSTRACT: It remains unknown whether plastic-biodegrading macroinvertebrates generate microplastics (MPs) and nanoplastics (NPs) during the biodegradation of plastics. In this study, we utilized highly sensitive particle analyzers and pyrolyzer-gas chromatography mass spectrometry (Py-GCMS) to investigate the possibility of generating MPs and NPs in frass during the biodegradation of polystyrene (PS) and low-density polyethylene (LDPE) foams by mealworms (*Tenebrio molitor* larvae). We also developed a digestive biofragmentation model to predict and unveil the fragmentation process of ingested plastics. The mealworms removed 77.3% of ingested PS and 71.1% of ingested PE over a 6-week test period. Biodegradation of both polymers was verified by the increase in the $\delta^{13}\text{C}$ signature of residual plastics, changes in molecular weights, and the formation of new oxidative functional groups. MPs accumulated in the frass due to biofragmentation, with residual PS and PE exhibiting the maximum percentage by number at 2.75 and 7.27 μm , respectively. Nevertheless, NPs were not detected using a laser light scattering sizer with a detection limit of 10 nm and Py-GCMS analysis. The digestive biofragmentation model predicted that the ingested PS and PE were progressively size-reduced and rapidly biodegraded, indicating the shorter half-life the smaller plastic particles have. This study allayed concerns regarding the accumulation of NPs by plastic-degrading mealworms and provided critical insights into the factors controlling MP and NP generation during macroinvertebrate-mediated plastic biodegradation.

KEYWORDS: Plastic biodegradation, Mealworms, Biofragmentation, Nanoplastics, Digestive model, $\delta^{13}\text{C}$ signature



INTRODUCTION

Microplastics (MPs, 10 μm to 5 mm) and nanoplastics (NPs, 1 to 1000 nm), derived from anthropogenic sources, now exist ubiquitously in the atmosphere, hydrosphere, and biosphere, with NPs further subdivided into nanosized plastics (1–100 nm) and submicro-MPs (100–1000 nm).^{1–7} Due to their unique properties, such as tiny size, large specific surface area, and high surface energy, MPs and NPs exhibit complex environmental behaviors and play a role in pollutant transport processes and biogeochemical cycling through multilateral interactions.^{5,8} Organisms in the aquatic and terrestrial environments are inevitably impacted by the MPs and NPs released from natural and anthropogenic sources. Researchers have elucidated the cell internalization of high-density polyethylene (HDPE) MPs (<80 μm) in the digestive system and their translocation to the bloodstream in the blue mussel (*Mytilus edulis* L.).⁹ Cytomembrane penetration by NPs has also been found to cause physiological and metabolic disorders, as well as growth retardation in animals.^{3,10} At present, MPs and NPs are considered emerging particulate

contaminants that pose a risk to human health through direct ingestion, inhalation, and accumulation in the human food web.¹

Ingestion of plastic debris by macroinvertebrates is widely observed in the natural environment, resulting in MPs commonly found in a variety of animals. The concern of biofragmentation of plastics debris into MPs, MPs into NPs by macrofauna, especially macroinvertebrates, has been addressed.¹¹ A study found that animal-based traditional medicinal materials contained polyethylene terephthalate (PET), polyethylene (PE), polypropylene (PP), and polyvinyl chloride (PVC) MPs.¹² Burrowing invertebrates also induce fragmentation of mariculture polystyrene (PS) floats, leading

Received: June 8, 2023

Revised: August 7, 2023

Accepted: September 6, 2023

Published: September 26, 2023



to the formation of MPs.¹³ The ingestion of plastics by macroinvertebrates is accompanied by biofragmentation behaviors via mouthparts and intestinal peristalsis, and smaller-sized plastic particles are typically generated.^{2,14–16} By microscopic observation, it was found that land snails (*Achatina fulica*) disintegrate and biofragment the ingested PS foam into PS MPs with a mean size of 1.343 ± 0.625 mm.¹⁷ However, it remains unclear whether NPs were generated and accumulated as a result of the method limit for particle detection, while the snails are capable of biodegrading PS. After Antarctic krill (*Euphausia superba*), which did not show PE biodegradation, ingested PE MPs ($31.5 \mu\text{m}$), the PE MPs were fragmented into smaller particles in their digestive gland, including NPs ranging from 150 to 500 nm.¹⁸ Freshwater amphipod *Gammarus duebeni* has been found to rapidly fragment PE MPs ($10\text{--}45 \mu\text{m}$) into a wide range of sizes, including NPs ranging from 558 nm to 1 μm , in digestive tracts.¹⁹ Earthworms (*Eisenia andrei*) exposed to two different sizes of PE MPs ($180\text{--}212 \mu\text{m}$ and $250\text{--}300 \mu\text{m}$) for 21 days also generated NPs ($180\text{--}364 \text{ nm}$) in their hindgut, which damaged the spermatogenesis and coelomocyte viability.²⁰ Characterization of ingested MPs in earthworm *Lumbricus terrestris* (Oligochaeta) indicated that the earthworms fragmented and depolymerized (or biodegraded) biodegradable polylactic acid (PLA) MPs ($300 \mu\text{m}$) and fragmented poly(butylene adipate-co-terephthalate) (PBAT) MPs ($234 \mu\text{m}$) and LDPE MPs ($362 \mu\text{m}$) into small-sized MPs ($20\text{--}113 \mu\text{m}$) without significant evidence supporting biodegradation.²¹ It remains unknown whether nanosized PLA and PBAT, both of which are biodegradable polymers, as well as LDPE particles, were generated. After ingestion by the aforementioned macroinvertebrates, these plastic fragments are excreted in the excrement (frass or fecula) and eventually enter ecosystems.^{22,23} Therefore, the digestive fragmentation of plastics by macroinvertebrates has been raised as a scientific concern. To date, research on the observation of NP generation and accumulation due to biofragmentation has primarily focused on targeted macroinvertebrates that lack plastic-degrading ability, such as Antarctic krill, earthworms, woodlice, and enchytraeids. Little is known about the digestive fragmentation behaviors of macroinvertebrates with exceptional plastic-degrading abilities during the biodegradation of plastics.

Recent studies have found that certain macroinvertebrates, especially insect larvae, are capable of the rapid biodegradation of plastics. Yellow mealworm, the larva of *Tenebrio molitor* Linnaeus 1758 (Coleoptera: Tenebrionidae) observed around the world and naturally present in forests with rotten wood, is one of the highly efficient plastic-degrading macroinvertebrates that voluntarily ingest a wide variety of petroleum-based plastic products, e.g., PS, low-density polyethylene (LDPE), polyurethane (PUR), PP, PVC, and PET.^{15,16,24–44} The unique metabolic process in the mealworm intestines endows them with great plastic-degrading capacities to depolymerize and biodegrade the ingested plastics through various gut-related mechanisms. After passing through the mealworm intestines, almost half of the ingested PS and LDPE can be efficiently biodegraded and mineralized within a short retention time of about 12 h, with residual polymers excreted in the frass.^{25,27–29,31,34,37,38,41,42,44–46} However, whether MPs or NPs are generated, retained, and accumulated as residues in the frass during the digestion of the plastics remains unknown. No detailed investigation has been conducted on the size

distribution of residual micro- and nanosized particles in the previously published reports due to a lack of methods for characterizing, predicting, and unveiling the digestive formation of MPs and NPs during plastic biodegradation.

In this study, we investigated the digestive fragmentation of commercial PS and LDPE foams by mealworms to assess the *in vivo* fate of the ingested plastics and determine the size distribution of residual plastic particles generated after biodegradation. We used highly sensitive particle-analyzing methods, i.e., laser light scattering sizer and pyrolyzer-gas chromatography mass spectrometry (Py-GCMS), to assess the size distribution of residual plastic particles and the mass content of potential NPs in frass. Additionally, we developed a digestive biofragmentation model based on enzymatic surface degradation to simulate the size-reduction process of plastic particles in the intestinal tract and compared the simulated results to the data of residual plastic particles detected with the sizer. Not only did we confirm the biodegradation of both PS and LDPE foams, supported by plastic mass balance, $\delta^{13}\text{C}$ signature changes, chemical modifications, and molecular-weight changes, but also we accurately detected the size distribution of residual plastic particles. We found that all of the residual plastics observed were within the MP range ($>2 \mu\text{m}$) without NPs detected above the detection limit ($>10 \text{ nm}$). Py-GCMS analyses showed negative results of NPs ($<100 \text{ nm}$) in the frass. We simulated the size-reduction processes of the ingested PS and PE particles in the intestinal tract using the digestive biofragmentation model. The predicted results aligned with the analytical results, indicating ultrafast biodegradation of small-sized plastic particles by mealworms. This study provided technically sound methodologies to test the size distribution of micro(nano)plastics and predict the digestive biofragmentation processes during macroinvertebrate-mediated plastic biodegradation.

MATERIALS AND METHODS

Source of Mealworms and Tested Plastic Feedstocks.

Yellow mealworms (or *T. molitor* larvae) were purchased from Binzhou Mealworm Co. (Binzhou, Shandong, China) and shipped overnight to our laboratory. The mealworms were 5–6 instars, with an average weight of $98.3 \pm 1.5 \text{ mg}$ (Table S1). The tested mealworms were not fed on any diets containing hormonal additives or antibiotics before, according to the dealer.

Expanded PS foam (density: 0.0207 g/cm^3 , CAS number: 9003-53-6) and LDPE foam (density: 0.0255 g/cm^3 , CAS number: 9002-88-4) were purchased from Zhonglian Petrochemical Co. (Guangdong, China) (Figures S1 and S2). The contents of 10 plasticizers commonly found in plastics were below the detection limits ($<0.05 \text{ ppm}$, w/w), indicating that the PS and LDPE foams are free from major additives (Table S2). The PS polymers had the number-average molecular weight (M_n) of $106.3 \pm 2.9 \text{ kDa}$, the weight-average molecular weight (M_w) of $338.5 \pm 8.4 \text{ kDa}$, and the size-average molecular weight (M_z) of $838.9 \pm 39.8 \text{ kDa}$. The LDPE polymer had a M_n of $41.3 \pm 6.1 \text{ kDa}$, a M_w of $152.8 \pm 3.1 \text{ kDa}$, and a M_z of $453.9 \pm 9.9 \text{ kDa}$ (Table S5). Both PS and PE fit the molecular weight range of commonly used plastic polymers (20 to 400 kDa).^{28,37}

Tetrahydrofuran (THF, GC grade purity $> 99.9\%$), ethanol (analytical grade), 1,2,4-trichlorobenzene (1,2,4-TCB, GC grade purity $> 99.9\%$), and other chemicals used in this

study were all purchased from Sigma-Aldrich Corporation in Shanghai, China.

Plastic Feeding Test. The mealworms were bred in glass containers (15 cm × 15 cm × 6 cm) with smooth inner surfaces. Each container initially contained 100 mealworms ($n = 3$) with either PS or LDPE foam (4.0 g). The experimental procedures and conditions followed established protocols as described in previous research 25, 26, 29, 33–35, 37, 38, 40, 41, and 47. The molted exoskeletons of mealworms and dead larvae were removed from the container daily to prevent any potential intraspecific diseases. To calculate plastic consumption and mass reduction, frass samples of mealworms were collected weekly over a six-week period. The weekly frass collection procedures were implemented under identical incubation conditions and did not cause any significant adverse effects on mealworm larvae, which previously demonstrated their capability and stability in plastic biodegradation.³³ All containers were maintained in a thermostatic incubator at a temperature of $25 \pm 0.5^\circ\text{C}$ and $70 \pm 5\%$ humidity.

PS and PE Mass Balance and Removal. To determine the mass balance and removal of ingested plastics by the mealworms, sequential extraction of frass samples was applied to weekly determine the water-extracted fraction (C_w), ethanol-extracted fraction (C_e), and solvent-extracted fraction (C_o ; THF for PS and 1,2,4-TCB for PE). The PS and PE removal was calculated based on the mass of plastics ingested by the mealworms, the mass of frass egested, and the residual polymer content in the frass (Text S1).^{15,30,36}

Analytical Methods for the Characterization of Plastic Biodegradation. The tested frass samples for characterizing PS and PE biodegradation were collected at the end of Week 6. At that time, the mealworms had reached the stable phase of plastic biodegradation. The mealworms were moved in separate clean glass containers overnight for frass collection as described previously.^{25,29,35,41}

Gel permeation chromatography (GPC, 1260 Infinity II GPC/SEC, Agilent Technologies Inc., U.S.A.) and high-temperature GPC (HT-GPC, 1260 Infinity II HT GPC, Agilent Technologies Inc., U.S.A.) analyses were conducted to determine the changes in the molecular weights (M_w , M_n , and M_z) of the ingested PS and LDPE polymers after biodegradation versus the virgin polymers as described previously (Text S2).^{28,37} The polydispersity index (PDI) was calculated as $\text{PDI} = M_w/M_n$. THF was used for PS extraction, and 1,2,4-TCB was used for PE extraction. All GPC analyses were performed in triplicate.

The ^{13}C stable isotope fraction in polymer samples was analyzed in order to identify the biodegradation of PS and LDPE foams. The elemental analyzer isotope ratio mass spectrometer (EA-IRMS, Vario EL cube-IsoPrime 100, Elementar, Germany) was employed to detect the modification of ^{13}C stable isotope signatures of the residual plastics from the frass versus the virgin plastic foam in delta ($\delta^{13}\text{C}$) notation in parts per thousand (‰) as follows:

$$\delta^{13}\text{C} (\text{\textperthousand}) = \left[\frac{(^{13}\text{C}/^{12}\text{C})_{\text{sample}}}{(^{13}\text{C}/^{12}\text{C})_{\text{standard}}} - 1 \right] \times 1000 \quad (1)$$

The $\delta^{13}\text{C}$ value was calibrated by the international carbon isotope standard Vienna Pee Dee Belemnite (VPDB). The overall precision of the ^{13}C measurement was $\pm 0.2\%$. The

analysis methods were referred to in previously published literature and described in Text S3.^{48–50,73}

To characterize the chemical modification of the ingested PS and PE polymers after passing through the larval intestines, attenuated total reflection Fourier transformed infrared spectroscopy (ATR-FTIR, Bruker tensor 27 FTIR spectrometer, Bruker, Optik, Germany) was applied to evaluate the oxidation and biodegradation of the ingested polymers.^{48,51,52} Before the test, the frass sample was placed in a drying oven for 24 h to remove any residual water that could cause analytical errors. The sample was subsequently placed on a platform and flattened with a glass slide for scanning and graphing (4000–500 cm^{-1}). OPUS software 7.0 (Bruker Optics, Germany) was used for processing the spectra.

Determination of Size Distribution and Examination of the Presence of Micro(nano)plastics. To determine the presence and size distribution of residual plastic particles belonging to micro- ($>10 \mu\text{m}$), submicro- ($100 \text{ nm}–10 \mu\text{m}$), and nanoplastics ($1 \text{ nm}–100 \text{ nm}$) in mealworm frass, the frass sample (3.0 g) at the end of the 6-week experiment was first mixed with a 30% H_2O_2 solution (wt/wt, 100 mL, specific gravity 1.1 g/mL) in a conical flask under gentle heating (70°C) conditions for at least 12 h to thoroughly digest organic matter. We used the mealworm frass at the end of the 6-week experiment for analysis because the mealworms have reached the stabilization phase of PS and PE biodegradation since Week 4. After the supernatant became clear, the solution containing residual plastic particles was allowed to stand for 1 h.^{15,53,54} The solution containing residual plastic particles underwent filtration using a polyamide (PA) membrane filter (porosity: 100 nm, Yibo Filter Material Co., Zhejiang, China), which was the most suitable filter with the smallest available pore size. The micro- and submicroplastic particles with a size exceeding 100 nm on the filter membrane were meticulously collected and observed under high vacuum conditions using a scanning electron microscope (SEM; Phenom Pro, Phenom World Inc., Netherlands). The size distribution of the filtered micro- and submicroplastic particles was measured via the laser light scattering sizer (Mastersizer 3000, Malvern Panalytical, UK) based on the particular volume with a measurement range of 0.01–3500 μm (Text S4). The accuracy of this method is better than the 0.6% variable, with a repeatability rate of over 99.9%. The relative particle percentage (RPP) or size distribution based on particle number was calculated by assuming that the particles were of spherical shape as follows

$$\text{RPP} = \frac{\text{VD}}{4/3\pi r^3} \times N \quad (2)$$

where RPP is the relative particle percentage (%); VD is the particular volume (%); r is the radius; and N is the normalization coefficient.

To examine whether NPs (size $<100 \text{ nm}$) were generated and accumulated in the frass, the filtrate was first evaporated to dryness in a crucible in the fume hood. After the filtrate was thoroughly dried, the solid residues of the filtrate were carefully collected. Finally, the plastic component in the solid residues (if any, size $< 100 \text{ nm}$) was quantified by pyrolyzer-gas chromatography mass spectrometry (Py-GCMS, 7890B-5977B GC/MS, Agilent Technologies Inc., U.S.A.). The calibration standard curves for the PS and PE polymers (Figure S3) were obtained using PS and PE standard substances (Agilent Technologies Inc., U.S.A.). The Py-GCMS method is a well-

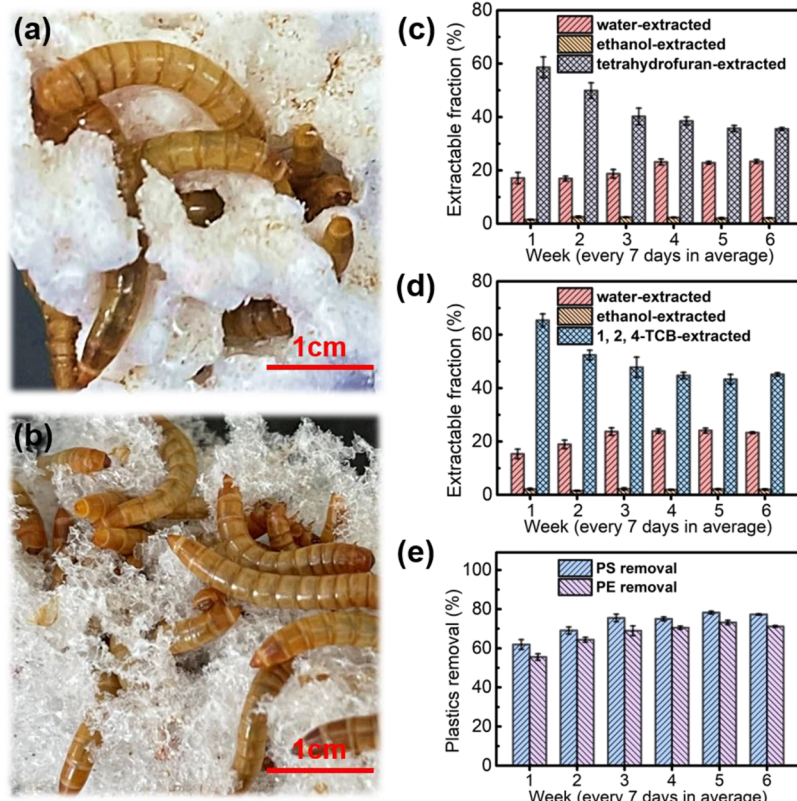


Figure 1. Characterization of ingestion of PS and LDPE foams by mealworms (*Tenebrio molitor* larvae). (a) PS foam-eating mealworms; (b) LDPE foam-eating mealworms; (c) the extracted fractions from the frass of the mealworms fed with PS foam on a weekly basis; (d) the extracted fractions from the frass of the mealworms fed with LDPE foam on a weekly basis; (e) the plastic removal efficiencies of PS and PE on a weekly basis. The frass samples from the mealworms fed with PS and LDPE foam were extracted by water, ethanol, and organic solvents (THF for PS and 1,2,4-TCB for LDPE).

established tool to quantify the content of plastic particles in human blood and animals.^{55–57}

Modeling the Digestive Biofragmentation Process.

To simulate the size-reduction process during the digestive biofragmentation of the ingested plastic particles, a digestive biofragmentation model for the size distribution of residual plastic particles on the basis of polymer volume was developed based on the following assumptions: a) The ingested plastic products enter the intestine through physical chewing and grinding via the mouthparts and intestinal peristalsis, and thus, the size of the plastic particles is less than the mouthparts; b) The biodegradation by the gut microbes and digestive enzymes reduces the size of the plastic particles; c) The physical grinding continues in the intestinal tract; d) Both biodegradation and grinding result in the biofragmentation of ingested plastic particles; e) The biofragmentation process is the function of the surface area of the particles;⁵⁸ and f) The biofragmentation and biodegradation kinetics follow a first-order reaction.^{59–64} In this study, the maximum initial size of the ingested plastics was assumed to be 450 μm , which corresponded to the size of the mouthparts of the mealworms tested. This value can change depending on the size or instar of the mealworms tested. According to the above assumptions, the size-reduction rate of the ingested plastics is a function of the size and specific surface area of particles, the grinding activity, and the biodegradation rate of the polymers within the intestinal microenvironment

$$\frac{dy_i}{dt} = - \left(k_1 \times A_i^\alpha + k_2 \times \frac{1}{A_i^\beta} \right) \times y_i \quad (3)$$

$$A_i = \frac{1}{R_i} \quad (4)$$

where $\frac{dy_i}{dt}$ is the volume reduction rate of the plastic particles with particle size i at time t (h); k_1 is the biodegradation rate constant of the plastics; k_2 is the grinding rate constant of the plastics; A_i is the instant specific surface area of the plastic particles with particle size i (nm^2); y_i is the quantity of the plastic particles; R_i is the diameter of the plastic particles with particle size i (nm); and α and β are the correction coefficients.

Matrix Laboratory (MATLAB 2022a, MathWorks Inc., U.S.A.) was used to calibrate the kinetic parameters for the digestive biofragmentation model.^{65,66} Specifically, the genetic algorithm was used to optimize the parameters k_1 , k_2 , α , and β with a population size of 24. The steps of the evolution algorithm are 10,000, with a crossover probability of 0.8 and a mutation probability of 0.8, according to the protocols of the genetic algorithm. As shown in eq 5, the fitness function is the sum of the absolute deviations of the experimental values obtained from the measured size distribution and the calculated values:

$$f = \sum_{i=1}^{85} |y_i - y_i^{obs}| \quad (5)$$

The digestive biofragmentation model was then applied to simulate the time courses of the size-reduction process of PS and PE particles with different initial particle sizes (i.e., 350, 300, 250, 200, 100, and 50 μm) in order to predict the size-frequency distribution of the particles and the removal efficiency of plastics. The detailed methodology for modeling the digestive biofragmentation is documented in *Text S5*.

Statistics Analysis and Quality Control. The significant differences in the extraction rates, plastic removal, and M_w , M_n , and M_z values were assessed by ANOVA and the student's *t* test with Tukey's correction.^{25,26,38} The Kolmogorov–Smirnov test (K–S test) was applied to determine whether the size distributions of the two MPs were significantly different. The statistical analyses were conducted by using SPSS (IBM, version 26.0). The significance level was set at 0.05, with all *p*-values adjusted. The data are the mean \pm standard deviations.

All experimental containers, vessels, and flasks were rinsed three times with Milli-Q ultrapure water and methanol (HPLC grade) to remove any potential background of micro- or nanoplastics. After thorough drying in the fume hood, the test materials and lab equipment were wrapped in aluminum foil and prepared for use.^{67,68} Before the filtration, Milli-Q ultrapure water was filtered through the membranes. The procedures of particle separation and identification were carried out in the fume hood in a dust-free clean room to prevent deviation caused by the indoor dust particles.

RESULTS AND DISCUSSION

Mass Balance and Removal of the Ingested Plastics by Mealworms. The mealworms aggressively masticated and ingested both the PS and PE foams in the container (*Figure 1a* and *1b*). The mass balance and removal of the ingested PS and PE plastics were monitored weekly based on the mass of the frass and residual plastic contents compared to the ingested plastics using the C_w , C_e , and C_o values of the frass samples (*Text S1*). The average frass yield, an indirect indicator of digestibility, was 0.65, 0.62, 0.61, 0.65, 0.61, and 0.64 mg of frass/mg of PS for the PS-fed mealworms and 0.68, 0.68, 0.65, 0.66, 0.62, and 0.64 mg of frass/mg of LDPE for the PE-fed mealworms in weeks 1, 2, 3, 4, 5, and 6, respectively (*Table S3*), indicating that a significant amount of the ingested PS and LDPE polymers was digested and mineralized.

The results of the C_w values indicated that the frass from both PS-fed and LDPE-fed mealworms contained a relatively high level of water-extracted fraction, which increased gradually from $17.1 \pm 2.1\%$ to $23.3 \pm 0.7\%$ for the PS frass and from $15.3 \pm 1.8\%$ to $23.3 \pm 0.3\%$ for the PE frass over the 6 weeks, respectively (*Figure 1c* and *1d*, *Table S3*). The C_w value represents the fraction of soluble organic components and salts in the frass.^{15,30} Therefore, the results implied that the ingested PS and LDPE foam were efficiently digested and hydrophilic soluble substances were generated.^{39,69} On the other hand, the water-extracted fraction of the frass samples both increased progressively during the first 4 weeks and stabilized after Week 4 (*Figure 1c* and *1d*, *Table S3*). The results suggested that the plastic-degrading ability of the mealworms was induced by feeding them plastics and reached its peak in 3–4 weeks. This is likely due to the enhancement of plastic-degrading microbial activities or specific functional microbial consortiums in the intestines during the first 4 weeks, thereby reaching the full ability of the biodegradation and mineralization of plastics. The ethanol-extracted fraction (the C_e value), which was used to determine ethanol soluble

intermediates in frass, was low in both PS and PE frass samples, varying between $1.5 \pm 0.1\%$ and $2.5 \pm 0.3\%$ (*Figure 1c* and *1d*, *Table S3*). This indicated that the ethanol-extractable substances generated were limited during PS and PE biodegradation.

The organic solvent-extracted fraction (the C_o value) represents the content of residual PS (extracted by THF) or residual PE (extracted by 1, 2, 4-TCB) in frass. The C_o values of the PS frass and PE frass both decreased gradually during the first 4 weeks, i.e., from $58.6 \pm 3.9\%$ to $38.5 \pm 1.5\%$ and from $65.4 \pm 2.4\%$ to $44.7 \pm 1.2\%$ from Week 1 to Week 4, respectively, and then stabilized (*Figure 1c* and *1d*, *Table S3*). The results indicated that the plastic degradation capacities of mealworms for both PS and LDPE increased and reached stable levels, resulting in the residual PS of less than 38.5% and the residual PE of less than 44.7% in the frass. This observation was similar to the changes in the THF extractable ratios of residual PS polymers during the PS biodegradation test by *T. molitor*³⁵ and *T. obscurus*²⁹ larvae.

Based on the results of the mass balance, the removal of PS and PE was calculated (*Figure 1e* and *Table S3*). Notably, the plastic removal or mass reduction was gradually increased from $61.9 \pm 2.5\%$ to $78.2 \pm 0.7\%$ for PS and from $55.5 \pm 1.7\%$ to $73.2 \pm 1.1\%$ for LDPE after Week 5. The results demonstrated that over 70% of the ingested PS and LDPE polymers were effectively digested and structurally decomposed in the gut microenvironment of mealworms, which fell within the previously reported range.^{25,34}

Depolymerization of the Ingested Plastics. GPC analysis was applied to characterize the polymer depolymerization during biodegradation of the ingested plastics by insects.^{33,38,70} As shown in *Figure 2a*, significant changes in the molecular weights (M_w , M_n , and M_z) of PS and PE polymers were observed by comparing the residual polymers with the respective original plastic foams. For the PS polymer, the M_w , M_n , and M_z were significantly reduced (*p* < 0.01) by $30.6 \pm 2.5\%$, $45.3 \pm 1.7\%$, and $32.7 \pm 3.8\%$, respectively, with the PDI value increasing from 3.18 ± 0.08 to 4.04 ± 0.18 (*Figure 2a* and *Table S4*), indicating a typical broad depolymerization pattern (BD) of PS, similar to previous reports.^{15,41,71} The PDI designates the heterogeneity in the chain-length distributions of tested polymers. Therefore, these data indicated that the polymer chains of PS were greatly reduced, and the broadness of the chain distribution increased after passage through the intestines, which was also similar to the biodegradation of commercial PS products by *Z. atratus* larvae (Coleoptera: Tenebrionidae).^{47,71}

The depolymerization of LDPE was different. The M_w , M_n , and M_z values of the residual PE polymers increased by $16.6 \pm 4.1\%$, $19.9 \pm 9.4\%$, and $34.4 \pm 6.9\%$, respectively, suggesting a limited-extent depolymerization pattern (LD) (*Figure 2a*), as observed previously during PE degradation in *T. molitor* and *Z. atratus* larvae.^{38,41,71} The LD in this study was likely attributed to the relatively high molecular weight of the LDPE foam used (M_w of 152.8 ± 3.1 kDa), since the BD of LDPE was observed during biodegradation of LDPE in mealworms using high purity LDPE with M_w of 0.64, 6.4, and 102.0 kDa.³⁷ Recent studies have found that the LD of the plastic polymers also occurred in mealworms during biodegradation of PS materials with a high molecular weight (i.e., 1,350 kDa)²⁸ and linear LDPE (LLDPE) and HDPE materials with a high branching and crystallinity degree.³⁷ On the other hand, the PDI of the residual PE polymers (3.67 ± 0.13) was also not significantly

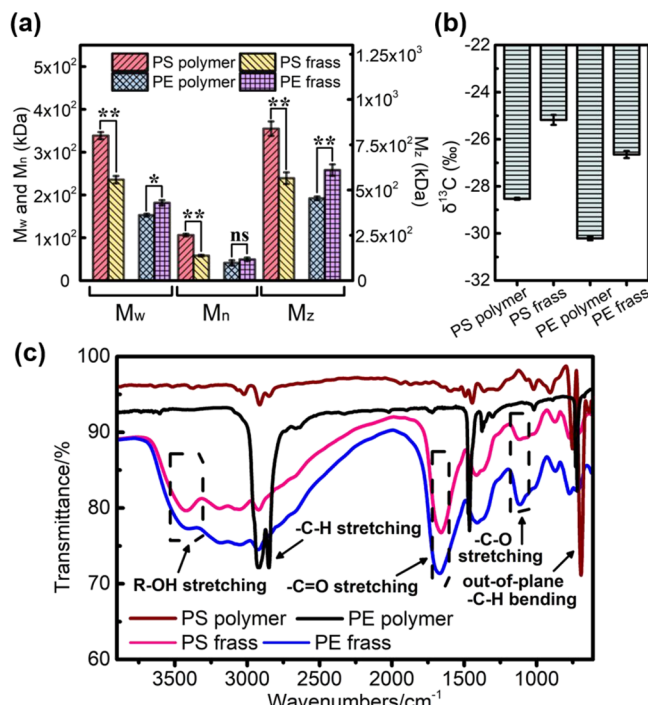


Figure 2. Characterization of biodegradation and oxidation of the ingested PS and LDPE polymers by the mealworms. (a) Changes in molecular weights (M_w , M_n , and M_z) of residual PS and LDPE versus original PS and LDPE polymers. ns indicates no significant difference. * indicates statistical significance $p < 0.05$, and ** indicates statistical significance $p < 0.001$. (b) $\delta^{13}\text{C}$ stable isotope signature of residual PS and LDPE foams. The overall precision of $\delta^{13}\text{C}$ measurement was $\pm 0.20\text{\textperthousand}$. (c) The FTIR spectra of the PS-fed and PE-fed frass versus the original PS and LDPE foam.

different ($p > 0.05$) from that of the original PE material (3.70 ± 0.08) (Table S4), implying that the broadness of polymer chain distribution remained mostly unchanged. Similar negligible changes in PDI have been reported in previous nonhydrolyzable plastic degradation studies using enzymes.^{5,72} This suggested that the random internal scission of midchains and long-chains in the polymer macromolecules yielded oligomeric products with a heterogeneous molecular weight distribution in the gut microenvironment of mealworms.^{58,72}

Evidence of Biodegradation of Plastics. In this study, we used $\delta^{13}\text{C}$ stable isotopic analysis to confirm the biodegradation of PS and LDPE by mealworms. During biodegradation, organisms preferentially take up light ^{12}C , and thus, the $\delta^{13}\text{C}$ signature of the residual polymers will be increased according to eq 1, depending on the metabolic pathway. The increase in the $\delta^{13}\text{C}$ stable isotope signatures indicated the chemical modifications due to biodegradation.^{49,50,73} The residual PS and PE particles in frass showed a significant increase in the $\delta^{13}\text{C}$ value from $-28.53 \pm 0.04\text{\textperthousand}$ to $-25.18 \pm 0.21\text{\textperthousand}$ and $-30.21 \pm 0.08\text{\textperthousand}$ to $-26.65 \pm 0.15\text{\textperthousand}$ ($p < 0.05$) compared to the virgin PS and PE polymers, respectively (Figure 2b and Table S5). The $\delta^{13}\text{C}$ stable isotopic analysis provided evidence of the biodegradation of PS and LDPE foam in mealworms and demonstrated that this method is a useful tool for the identification of insect-mediated plastic biodegradation.

Oxidation and biodegradation of the ingested PS and LDPE polymers were identified by ATR-FTIR. New indicative functional groups appeared in the FTIR spectra of the frass

samples derived from both PS-fed and PE-fed mealworms (Figure 2c), including C–O stretching ($1050\text{--}1150\text{ cm}^{-1}$), C=O stretching (1700 cm^{-1}), and R–OH stretching ($2500\text{--}3500\text{ cm}^{-1}$). The presence of the R–OH stretching vibrations revealed that the degradation in the mealworm gut significantly improved the hydrophilicity of the ingested PS and PE polymers.^{16,17} The incorporation of oxygen atoms in the polymer backbone corroborated the oxidation and biodegradation of the ingested plastics in the intestines.^{15,74}

Characterization of the Size Distribution of Residual Plastics in Frass. The morphotypes of the original plastic foams and the residual PS and PE particles in the foam at the end of the 6-week experiment were observed using SEM (Figures 3 and S2). After biodegradation, the PS and LDPE foams (Figure 3a and 3b inset) were fragmented into microsized particles of different sizes and irregular morphotypes, and most of the plastic particles were serrated (Figure 3a and 3b). The SEM images indicated that the digestive biofragmentation of the ingested plastics occurred in the intestines of mealworms. As observed, the residual PS particles were slightly smaller than the residual PE particles (Figure 3a and 3b).

The size distribution of residual micro- and submicroplastic particles was further measured using the laser light scattering sizer (Figure 3c to 3f), with a measurement range of 0.01 to $3500\text{ }\mu\text{m}$ for the samples at the end of Week 1 (Figure 3c and 3d) and Week 6 (Figure 3e and 3f). As observed in SEM images, the overall size of the residual PS particles in frass was smaller than that of the residual PE particles at both the end of Week 1 and Week 6, with respective peak volume percentages reaching $126.65\text{ }\mu\text{m}$ versus $239.78\text{ }\mu\text{m}$ on Week 1 and $88.35\text{ }\mu\text{m}$ versus $211.04\text{ }\mu\text{m}$ on Week 6 for PS and PE MPs, respectively (Figure 3c and 3e). The smaller peak size of PS could be associated with a relatively higher removal efficiency of PS than LDPE (e.g., 61.9% versus 55.5% in Week 1 and 77.3% vs 71.1% in Week 6) in this study (Tables S3).

Based on the results of polymer volume-based particle size distribution (Figure 3c and 3e), the size distribution of particles based on particular number was further estimated by assuming a spherical shape of the particles.^{15,75,76} The results showed that the size of the most abundant residual particles was 2.69 and $3.55\text{ }\mu\text{m}$, respectively, in PS frass and PE frass at the end of Week 1 (Figure 3d). This size increased to 2.75 and $7.27\text{ }\mu\text{m}$ in PS and PE frass, respectively, at the end of Week 6 (Figure 3f). The smaller residual particle size based on the particular number at the end of Week 1 compared to that of Week 6 could be associated with the progressive increase in biodegradation ability of the mealworms, which resulted in better removal of smaller-sized particles at the end of Week 6 compared to Week 1. These findings also suggested that the ingested plastics were partially digested and mineralized in the intestine of mealworms, with the size of particles influenced by the mealworm's digestibility. Data analysis indicated that the smallest particles detected were 2.09 and $3.11\text{ }\mu\text{m}$ at the end of Week 1 and 2.42 and $5.92\text{ }\mu\text{m}$ at the end of Week 6 for PS and PE in the frass, respectively, which were well above the detection limit of the laser light scattering sizer of $0.01\text{ }\mu\text{m}$ (10 nm), indicating that NPs were not detected within the measurement range in all frass samples (Figure 3d and 3f). These results suggested that nanosized PS and PE particles ($<2\text{ }\mu\text{m}$) did not significantly accumulate or were generated well below detection limit, if any were present, in the frass during the biodegradation of PS and LDPE foams by mealworms.

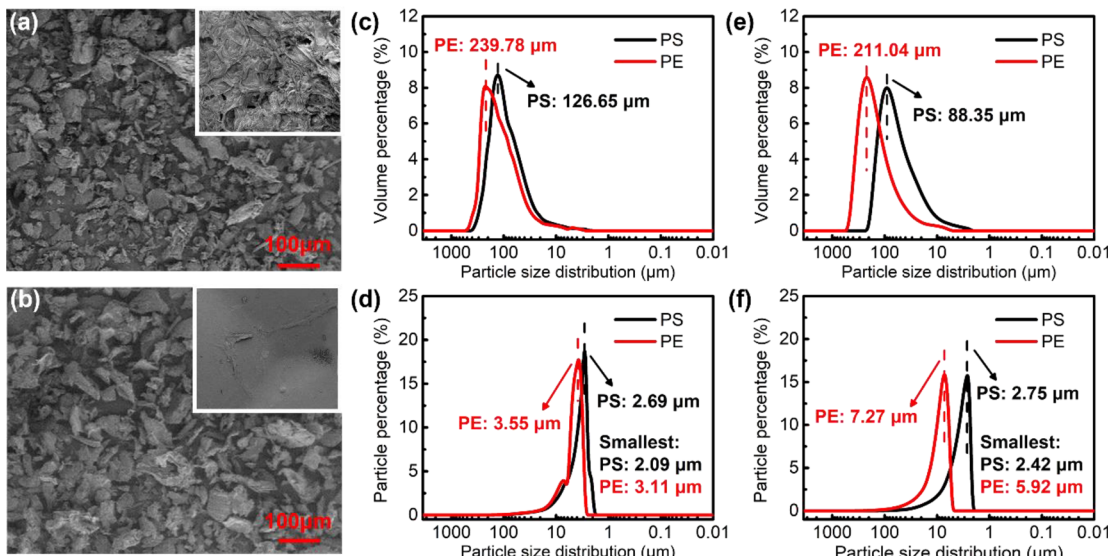


Figure 3. Characterization of the size-frequency distribution of residual plastics in frass. (a) The SEM image of PS foam (inserted) and residual PS particles separated from the frass of mealworms fed with PS foam at the end of Week 6. The inset figure shows the surface morphology of the original plastic foam. (b) The SEM image of LDPE foam (inserted) and residual PE particles separated from the frass of mealworms fed with LDPE foam at the end of Week 6. The volume-based size-frequency distribution of residual PS and PE particles separated from the frass of mealworms fed with PS foam and LDPE foam (c) at the end of Week 1, with the peak volume size achieved at 126.65 and 239.78 μm , respectively, and (e) at the end of Week 6, with the peak volume size achieved at 88.35 and 211.04 μm for PS and PE, respectively. The particle number-based size-frequency distribution of residual PS and PE particles separated from the frass of mealworms fed with PS foam and LDPE foam (d) at the end of Week 1, with the peak number sizes achieved at 2.69 and 3.55 μm for PS and PE, respectively (the minimum detected size: PS, 2.09 μm ; LDPE, 3.11 μm), and (f) at the end of Week 6, with the peak number sizes achieved at 2.75 and 7.27 μm for PS and PE, respectively (the minimum detected size: PS, 2.42 μm ; LDPE, 5.92 μm).

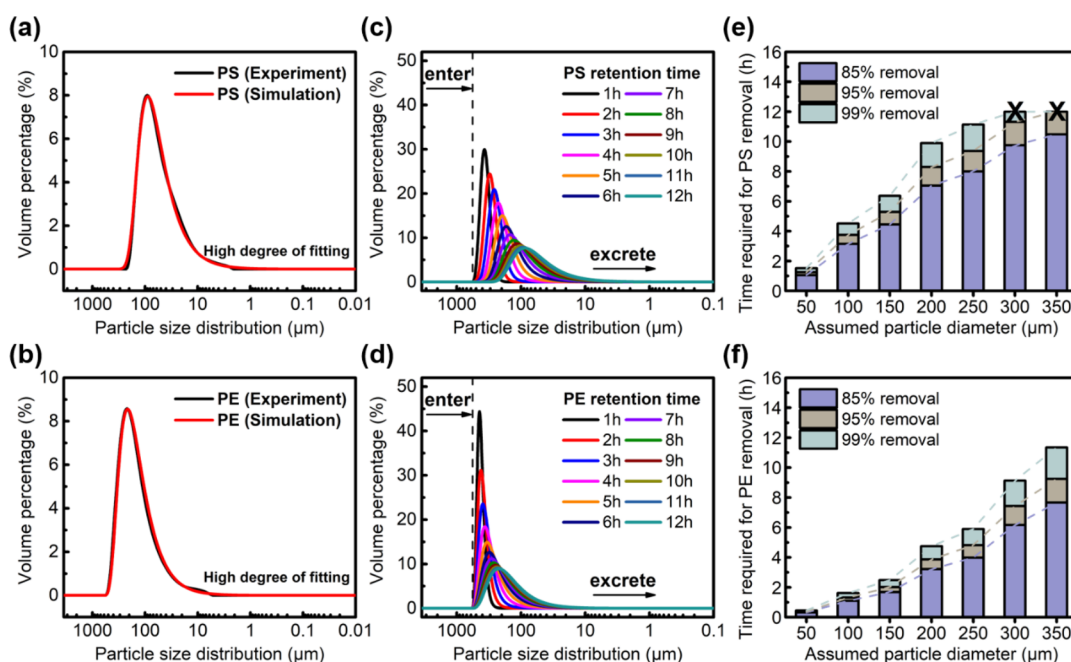


Figure 4. Digestive biofragmentation modeling of the size-reduction process of the ingested PS and PE plastic particles in mealworms. (a) The simulated size-frequency particle distribution of residual PS polymer by MATLAB versus the size distribution measured by the laser light scattering particle sizer and (b) the simulated size-frequency particle distribution of residual PE polymer by MATLAB versus the size distribution measured by the laser light scattering particle sizer. The simulated time course of the size-frequency distribution of the ingested (c) PS and (d) PE from 1 to 12 h in the larval intestine. (e) The estimated time required for the removal of different-sized PS microplastics and (f) the estimated time required for the removal of different-sized PE microplastics. The particle sizes (μm) were set at 350, 300, 250, 200, 100, and 50 μm .

On the particular volume basis, the peak size of residual particles of both PS and PE decreased from Week 1 to Week 6. This is consistent with the progressive increase in plastic

removal efficiency (Figure 1e). The peak size on the basis of particle number for PS was maintained at around 2.7 μm , while that for PE was increased from 3.55 to 7.27 μm from Week 1

to Week 6. The reason for the size distribution change for PE particles was not clear and could be related to polymer biodegradability and physical properties (crystallinity, rigidity, branching, etc.) of PE polymer. Future research is needed.

Detection of NP Contents in Frass. Py-GCMS analysis was employed to determine whether residual nanosized plastic particles (if any, nominally <100 nm) significantly accumulated in the frass suspension after filtration through a PA membrane with a pore size of 100 nm, using established methods.⁵⁶ The calibration standard curves were obtained by using PS and PE standard polymers (Figure S3). The Py-GCMS method is a well-established tool to quantify the content of plastic particles in human blood and animals.^{55–57} The analytical results showed that the contents of PS and PE components in the filtrate derived from the PS and PE frass via a PA membrane were both below the detection limit (Table S6), i.e., the plastics contents (w/w) were approximately less than 0.00029 ppm for PS or 0.0014 ppm for PE in their respective frass. This indicated that NPs were basically absent or at least did not significantly accumulate in the frass samples if they were generated, as determined by the highly sensitive particle sizer (Figure 3). The results also supported the ultrafast removal capacity of small-sized plastic particles by the mealworms during PS and LDPE biodegradation.

Modeling of Digestive Size-Reduction Process. The digestive biofragmentation model of ingested PS and LDPE was established using MATLAB based on the degradation and grinding hypotheses and the size distribution of residual plastic particles in frass. The initial particle size of the ingested plastics was assumed to be 450 μm , and the retention time in the mealworm intestine was set at 12 h, which is consistent with previous research that reports mealworm larvae typically require approximately 12 h to complete foam digestion and excrete the frass residue.^{25,26,29,33} The genetic algorithm was employed to determine the optimized parameters (k_1, k_2, α , and β) for both PS and PE polymers (Table S7).

The simulated particle size distribution of the residual plastics, obtained by MATLAB, fitted well with the results measured by the laser light scattering sizer at the end of Week 6 under stabilized biodegradation conditions (Figure 4a and 4b). The findings demonstrate that the digestive biofragmentation model is appropriate for estimating the digestive size-reduction processes and biodegradation and removal of the ingested PS and PE plastic particles. As shown in Table S7, the PS and PE polymers exhibited significantly different biodegradation rates (k_1) and grinding rates (k_2) during the size-reduction processes.

Using the kinetic parameters obtained, further simulations were performed to predict the time course of the size-frequency distribution of plastic particles at various retention times (from 1 to 12 h). As shown in Figure 4c and 4d, both ingested PS and PE underwent size-reduction processes in the intestines of the larvae prior to excretion, as predicted using the digestive biofragmentation model. Overall, the size-frequency distribution of the particles gradually shifted from a higher mean size to a lower mean size as the retention time elapsed toward excrement (Figure 4c and 4d). The PE particles had a larger mean size at 1 h than the PS particles initially. However, the mean size of the PE particles decreased faster than the PS particles due to higher k_1 (304.6 vs 37.6) and k_2 (1.71 vs 1.47) of LDPE compared to PS (Table S7). After approximately 12 h of gut retention time, undigested plastic particles of different sizes were excreted as frass residue.

The established digestive biofragmentation model was further applied to estimate the time required for the removal of different-sized PS and PE particles with initial fixed sizes (μm) of 350, 300, 250, 200, 100, and 50 by 85%, 95%, and 99%. The predicted results indicated that all PS and PE MPs with initial sizes smaller than 250 μm could be completely digested and removed (>99% removal) within 12 h of retention time (Figure 4e and 4f), if they were ingested by mealworms. The smaller the particle size, the shorter the retention time required to achieve complete digestive removal. For instance, the complete removal of MPs with an initial diameter of 50 μm would take less than 1 h. Using the predicted results, the half-life time ($t_{1/2}$) of plastic plastics (or the time required for number reduction to half of the initial value) with different sizes was estimated, which further confirmed that the smaller the size, the shorter the $t_{1/2}$ (Figure S4). The simulations explain why the NPs were well below the detection limit in the frass of the mealworms fed with PS or LDPE foam. For example, the $t_{1/2}$ values of 50 μm PS and PE particles were only about 47 and 14 min, respectively (Table S8). After 12 h of retention time, the remaining percentage (R) values of PS and PE particles with 50 μm would be only 0.0024% and $3.3 \times 10^{-14}\%$, respectively. The nanosized particles would have much shorter $t_{1/2}$ values and would be rapidly removed within much shorter retention time. A recent study on PS biodegradation by PS-degrading *Galleria mellonella* larvae by Wang et al. (2022) indicated that after 48 h of force-feeding the larvae with PS MPs (diameter 25 μm) labeled with red-fluorescence, the fluorescent intensities declined significantly by 27%, 56%, 66%, and 80% at 3, 6, 12, and 18 h, respectively,⁷⁷ and no fluorescent intensity was detected at 24 h. After the injection of PS microbeads with a size of 200 mesh (or 74 μm) into the *Galleria mellonella* larvae, the size of the PS microbeads decreased significantly at 6 h and completely disappeared at 24 h using SEM observation. The results supported that small PS MPs (74 μm or less) can be completely removed or digested in plastic-degrading insect larvae, as predicted by our digestive biofragmentation model.

The ultrafast biodegradation of PS and PE, especially for small particles, is likely the result of synergistic bioreactions between the host and gut microbes. The intestinal tissues of *T. molitor* larvae secreted emulsifying components of 30–100 kDa, which mediated PS bioavailability, and the intestinal microbial community also produced substances of <30 kDa that increased microbiological respiration and thus collaborated to achieve highly efficient plastic biodegradation.²⁴ Given the plastic-digesting ability and gut microbiological conversion capacity of the mealworms, small plastic particles (e.g., in nano- or submicrometer-sized) with high specific surface (i.e., the ratio of surface area to volume or surface area to polymer mass) and surface reaction energy would be eliminated at an ultrafast speed through enzymatic and microbial reactions without significant accumulation.

The findings in this study suggest that the frass or excrement from mealworm-mediated biodegradation of plastic products (such as PS and PE foam) is relatively environmentally and biologically free of concern about NP accumulation since small-sized plastic particles are unable to significantly accumulate in the excrement. Similar hypotheses could be drawn for other macroinvertebrates with remarkable plastic-degrading capacities, such as *Tenebrio obscurus* larvae,³⁶ *Zophobas atratus* larvae,^{15,38} *Plesiophthalmus davidi*,⁷⁸ *Uloma* sp.,⁷⁹ *Achroia grisella*,⁸⁰ and *Galleria mellonella* larvae,^{51,77,81} as

well as land snails (*Achatina fulica*).¹⁷ This hypothesis has been supported by a recent report on the complete digestion of PS MPs (<75 µm) in the gut of PS-degrading *G. mellonella* larvae (Lepidoptera: Pyralidae) after 48 h of force-feeding.⁷⁷ Further research is still needed to confirm this hypothesis with different plastic-degrading macroinvertebrates and major commercial plastic products including LDPE, HDPE, PP, PVC, PS, PET, and PUR.

Environmental Implications. Based on the results of this study, we conclude that macroinvertebrates without or with poor plastic-degrading ability, e.g., Antarctic krill, freshwater amphipod, and earthworms, biofragment the ingested MPs into NPs.^{18,21} Rapid plastic-degrading macroinvertebrates, e.g., mealworms (*T. molitor* larvae), also biofragment the ingested plastic foam products into smaller-sized MPs, but accumulation of nanosized plastic particles in the frass (excrement) was not observed and not detected using highly sensitive detection methods, i.e., laser light scattering sizer and Py-GC/MS analysis. The results are explained by digestive biofragmentation modeling.

In this study, we also confirmed for the first time the biodegradation of commercial PS and LDPE foam in mealworms by determining the $\delta^{13}\text{C}$ signature of the residual PS or PE in frass versus the original PS or LDPE foams. This was based on the fact that organisms preferentially take up the light isotope ^{12}C , resulting in an increased $\delta^{13}\text{C}$ signature in the residual plastics due to bioreaction. This method will provide another useful and effectively scientific tool to assess the biodegradation of commercial plastics in macroinvertebrates as well as by microorganisms.

This work utilized the highly sensitive laser light scattering sizer combined with Py-GC/MS analysis to accurately determine the size distribution of residual plastic particles after biodegradation of commercial PS and LDPE foams on a volume basis and to estimate the particle distribution on a number basis. The results demonstrated that the ingested plastic foams were biofragmented into MPs larger than 2 µm, but NPs were not detected above the detection limit in the frass. These results dispel our major concerns about the significant accumulation of NPs in frass during the insect-mediated biodegradation of commercial plastic products because NPs, as emerging tiny particulate contaminants, pose greater environmental and biological risks in natural ecosystems than MPs. Future studies will be performed to further verify the absence of NPs by looking for extremely sensitive tools to assess the residual polymer content lower than the detection limits of the current tools used.

The simulated size-frequency distribution of plastic particles using the digestive biofragmentation model developed in this study highly fit the data measured by the laser particle analyzers. Further simulation using this model reveals that the ingested PS and PE polymers underwent progressive size-reduction processes under biodegradation as they passed through the intestinal tract. The digestive biofragmentation model also indicates that the size distribution of residual particles and plastic removal are functions of the retention time and initial size of the plastic particles. The simulation results are consistent with the analytical results; i.e., the ingested polymers were removed by more than 70% after digestion in the mealworm gut, and small-sized particles were removed or biodegraded at an ultrafast speed. Based on these findings, we hypothesize that nanosized plastic particles are unlikely to accumulate in the frass of macroinvertebrates that have high

plastic-degrading capacities. Other insect larvae with similar plastic-degrading features to mealworms, e.g., *Zophobas atratus*,¹⁵ *Tenebrio obscurus*,^{29,36} *G. mellonella* larvae,^{51,77,81,82} *Plesiophthalmus davidi*,⁷⁸ and *Uloma* sp.,⁷⁹ as well as land snails,¹⁷ need to be further tested using different commercial plastic products and high purity plastics.

ASSOCIATED CONTENT

Supporting Information

The Supporting Information is available free of charge at <https://pubs.acs.org/doi/10.1021/acs.est.3c04406>.

5 additional supporting methods (Texts S1–S5), the Commercial PS and LDPE materials used in this study (Figure S1); the SEM image of the surface of original PS and PE foam (Figure S2); detection of the plastic content (nanoplastics) in the filtrate after digestion (Figure S3); simulation results of half-life periods of ingested plastics using the established digestive biofragmentation model (Figure S4); specific physiological features of the tested mealworms (Table S1); plasticizer contents in tested PS and PE foams according to GC-MS analysis (Table S2); characterization of frass using sequential extractions and plastic removal by weekly basis (Table S3); the results of GPC analysis (Table S4); the results of the $\delta^{13}\text{C}$ of stable isotope test for the frass (Table S5); the results of the analysis of the plastic content in the filtrate with Py-GC/MS (Table S6); the kinetic parameters of the digestive fragmentation model optimized with MATLAB (Table S7); and the simulation results of the half-life time ($t_{1/2}$) of ingested plastics with different initial sizes (Table S8) (PDF)

AUTHOR INFORMATION

Corresponding Authors

Wei-Min Wu – Department of Civil and Environmental Engineering, William & Cloy Codiga Resource Recovery Center, Stanford University, Stanford, California 94305-4020, United States; orcid.org/0000-0001-5244-0655; Phone: +1650-7245310; Email: Billwu@stanford.edu

Yalei Zhang – State Key Laboratory of Pollution Control and Resource Reuse, College of Environmental Science and Engineering, Tongji University, Shanghai 200092, China; orcid.org/0000-0002-3254-8965; Phone: +86 21 65985811; Email: Zhangyalei@tongji.edu.cn

Authors

Bo-Yu Peng – State Key Laboratory of Pollution Control and Resource Reuse, College of Environmental Science and Engineering, Tongji University, Shanghai 200092, China

Shaoze Xiao – State Key Laboratory of Pollution Control and Resource Reuse, College of Environmental Science and Engineering, Tongji University, Shanghai 200092, China

Ying Sun – State Key Laboratory of Pollution Control and Resource Reuse, College of Environmental Science and Engineering, Tongji University, Shanghai 200092, China

Yurong Liu – Key Laboratory of Smart Manufacturing in Energy Chemical Process, Ministry of Education, East China University of Science and Technology, Shanghai 200237, China; orcid.org/0000-0001-6893-3913

Jiabin Chen – State Key Laboratory of Pollution Control and Resource Reuse, College of Environmental Science and

Engineering, Tongji University, Shanghai 200092, China;
 ⓘ orcid.org/0000-0002-4790-5873
Xuefei Zhou – State Key Laboratory of Pollution Control and Resource Reuse, College of Environmental Science and Engineering, Tongji University, Shanghai 200092, China;
 ⓘ orcid.org/0000-0001-6521-0592

Complete contact information is available at:
<https://pubs.acs.org/10.1021/acs.est.3c04406>

Author Contributions

B.-Y.P. and S.X. contributed equally to this work.

Notes

The authors declare no competing financial interest.

ACKNOWLEDGMENTS

This work was financially supported by the National Natural Science Foundation of China (No. U21A20322), the Shanghai Science and Technology Innovation Action Plan (No. 22dz1205700), the Fundamental Research Funds for the Central Universities (No. 2022-4-ZD-05), and the China Baowu Low Carbon Metallurgy Innovation Foundation (No. BWLCF202105). We also gratefully acknowledge support from the Woods Institute for Environment at Stanford University (Award 1197667-10-WTAZB). We thank Professor Craig S. Criddle, Stanford University for the suggestions during this study. We also thank Xiaoling Ye from Shiyanjia Lab (www.shiyanjia.com) for the figure preparation.

NOMENCLATURE

ATR-FTIR	Attenuated total reflection fourier transformed infrared spectroscopy
BD	Broad depolymerization
C _e	Ethanol-extracted fraction
C _o	Organic solvent-extracted fraction
C _w	Water-extracted fraction
EA-IRMS	Elemental analyzer isotope ratio mass spectrometer
FTIR	Fourier transform infrared spectroscopy
GPC	Gel permeation chromatography
HDPE	High-density polyethylene
LD	Limited-extent depolymerization
LDPE	Low-density polyethylene
MPs	Microplastics
M _n	Number-average molecular weight
M _w	Weight-average molecular weight
M _z	Size-average molecular weight
MWD	Molecular weight distribution
NPs	Nanoplastics
1,2,4-TCB	1,2,4-Trichlorobenzene
PA	Polyamide
PBAT	Poly(butylene adipate-co-terephthalate)
PDI	Polydispersity index
PE	Polyethylene
PET	Polyethylene terephthalate
PLA	Polylactic acid
PP	Polypropylene
PS	Polystyrene
PUR	Polyurethane
PVC	Polyvinyl chloride
Py-GCMS	Pyrolyzer-gas chromatography mass spectrometry
PPP	Relative particle percentage
SEM	Scanning electron microscope

SPCR	Specific PS consumption rate
SR	Survival rate
THF	Tetrahydrofuran
VPDB	Vienna Pee Dee Belemnite

REFERENCES

- (1) Allen, D.; Allen, S.; Abbasi, S.; Baker, A.; Bergmann, M.; Brahney, J.; Butler, T.; Duce, R. A.; Eckhardt, S.; Evangelou, N.; et al. Microplastics and nanoplastics in the marine-atmosphere environment. *Nat. Rev. Earth Env.* **2022**, *3* (6), 393–405.
- (2) Wang, L.; Wu, W.-M.; Bolan, N. S.; Tsang, D. C. W.; Li, Y.; Qin, M.; Hou, D. Environmental fate, toxicity and risk management strategies of nanoplastics in the environment: Current status and future perspectives. *J. Hazard. Mater.* **2021**, *401*, No. 123415.
- (3) Xiao, F.; Feng, L. J.; Sun, X. D.; Wang, Y.; Wang, Z. W.; Zhu, F. P.; Yuan, X. Z. Do polystyrene nanoplastics have similar effects on duckweed (*Lemna minor* L.) at environmentally relevant and observed-effect concentrations? *Environ. Sci. Technol.* **2022**, *56* (7), 4071–4079.
- (4) Zhang, S.; He, Z.; Wu, C.; Wang, Z.; Mai, Y.; Hu, R.; Zhang, X.; Huang, W.; Tian, Y.; Xia, D.; et al. Complex bilateral interactions determine the fate of polystyrene micro- and nanoplastics and soil protists: Implications from a soil amoeba. *Environ. Sci. Technol.* **2022**, *56* (8), 4936–4949.
- (5) Min, K.; Cuiffi, J. D.; Mathers, R. T. Ranking environmental degradation trends of plastic marine debris based on physical properties and molecular structure. *Nat. Commun.* **2020**, *11* (1), 727.
- (6) Bermudez, J. R.; Swarzenski, P. W. A microplastic size classification scheme aligned with universal plankton survey methods. *MethodsX* **2021**, *8*, No. 101516.
- (7) Hartmann, N. B.; Huffer, T.; Thompson, R. C.; Hassellov, M.; Verschoor, A.; Daugaard, A. E.; Rist, S.; Karlsson, T.; Brennholt, N.; Cole, M.; et al. Are we speaking the same language? Recommendations for a definition and categorization framework for plastic debris. *Environ. Sci. Technol.* **2019**, *53* (3), 1039–1047.
- (8) Wang, J.; Li, J.; Wang, Q.; Sun, Y. Microplastics as a vector for HOC bioaccumulation in earthworm *Eisenia fetida* in soil: Importance of chemical diffusion and particle size. *Environ. Sci. Technol.* **2020**, *54* (19), 12154–12163.
- (9) von Moos, N.; Burkhardt-Holm, P.; Kohler, A. Uptake and effects of microplastics on cells and tissue of the blue mussel *Mytilus edulis* L. after an experimental exposure. *Environ. Sci. Technol.* **2012**, *46* (20), 11327–11335.
- (10) Sanchez-Hernandez, J. C. A toxicological perspective of plastic biodegradation by insect larvae. *Comp. Biochem. Physiol. C Toxicol. Pharmacol.* **2021**, *248*, No. 109117.
- (11) So, M. W. K.; Vorsatz, L. D.; Cannicci, S.; Not, C. Fate of plastic in the environment: From macro to nano by macrofauna. *Environ. Pollut.* **2022**, *300*, 118920.
- (12) Lu, S.; Qiu, R.; Hu, J.; Li, X.; Chen, Y.; Zhang, X.; Cao, C.; Shi, H.; Xie, B.; Wu, W. M.; et al. Prevalence of microplastics in animal-based traditional medicinal materials: Widespread pollution in terrestrial environments. *Sci. Total Environ.* **2020**, *709*, No. 136214.
- (13) Zheng, Y.; Zhu, J.; Li, J.; Li, G.; Shi, H. Burrowing invertebrates induce fragmentation of mariculture Styrofoam floats and formation of microplastics. *J. Hazard. Mater.* **2023**, *447*, No. 130764.
- (14) Gaylarde, C. C.; Baptista Neto, J. A.; da Fonseca, E. M. Nanoplastics in aquatic systems - are they more hazardous than microplastics? *Environ. Pollut.* **2021**, *272*, No. 115950.
- (15) Peng, B.-Y.; Sun, Y.; Wu, Z.; Chen, J.; Shen, Z.; Zhou, X.; Wu, W.-M.; Zhang, Y. Biodegradation of polystyrene and low-density polyethylene by *Zophobas atratus* larvae: Fragmentation into microplastics, gut microbiota shift, and microbial functional enzymes. *J. Clean. Prod.* **2022**, *367*, No. 132987.
- (16) Wang, Y.; Luo, L.; Li, X.; Wang, J.; Wang, H.; Chen, C.; Guo, H.; Han, T.; Zhou, A.; Zhao, X. Different plastics ingestion preferences and efficiencies of superworm (*Zophobas atratus* Fab.) and yellow mealworm (*Tenebrio molitor* Linn.) associated with

- distinct gut microbiome changes. *Sci. Total Environ.* **2022**, *837*, No. 155719.
- (17) Song, Y.; Qiu, R.; Hu, J.; Li, X.; Zhang, X.; Chen, Y.; Wu, W.-M.; He, D. Biodegradation and disintegration of expanded polystyrene by land snails *Achatina fulica*. *Sci. Total Environ.* **2020**, *746*, No. 141289.
- (18) Dawson, A. L.; Kawaguchi, S.; King, C. K.; Townsend, K. A.; King, R.; Huston, W. M.; Bengtson Nash, S. M. Turning microplastics into nanoplastics through digestive fragmentation by Antarctic krill. *Nat. Commun.* **2018**, *9* (1), 1001.
- (19) Mateos-Cardenas, A.; O'Halloran, J.; van Pelt, F.; Jansen, M. A. K. Rapid fragmentation of microplastics by the freshwater amphipod *Gammarus duebeni* (Lillj.). *Sci. Rep.* **2020**, *10* (1), 12799.
- (20) Kwak, J. I.; An, Y. J. Microplastic digestion generates fragmented nanoplastics in soils and damages earthworm spermatogenesis and coelomocyte viability. *J. Hazard. Mater.* **2021**, *402*, No. 124034.
- (21) Meng, K.; Lwanga, E. H.; van der Zee, M.; Munhoz, D. R.; Geissen, V. Fragmentation and depolymerization of microplastics in the earthworm gut: A potential for microplastic bioremediation? *J. Hazard. Mater.* **2023**, *447*, No. 130765.
- (22) Ni, B.-J.; Zhu, Z.-R.; Li, W.-H.; Yan, X.; Wei, W.; Xu, Q.; Xia, Z.; Dai, X.; Sun, J. Microplastics mitigation in sewage sludge through pyrolysis: The role of pyrolysis temperature. *Environ. Sci. Technol. Lett.* **2020**, *7* (12), 961–967.
- (23) Azeem, I.; Adeel, M.; Ahmad, M. A.; Shakoor, N.; Zain, M.; Yousef, N.; Yinghai, Z.; Azeem, K.; Zhou, P.; White, J. C.; et al. Microplastic and nanoplastic interactions with plant species: Trends, meta-analysis, and perspectives. *Environ. Sci. Technol. Lett.* **2022**, *9* (6), 482–492.
- (24) Brandon, A. M.; Garcia, A. M.; Khlystov, N. A.; Wu, W. M.; Criddle, C. S. Enhanced bioavailability and microbial biodegradation of polystyrene in an enrichment derived from the gut microbiome of *Tenebrio molitor* (mealworm larvae). *Environ. Sci. Technol.* **2021**, *55* (3), 2027–2036.
- (25) Brandon, A. M.; Gao, S. H.; Tian, R.; Ning, D.; Yang, S. S.; Zhou, J.; Wu, W.-M.; Criddle, C. S. Biodegradation of polyethylene and plastic mixtures in mealworms (larvae of *Tenebrio molitor*) and effects on the gut microbiome. *Environ. Sci. Technol.* **2018**, *52* (11), 6526–6533.
- (26) Brandon, A. M.; El Abbadi, S. H.; Ibekwe, U. A.; Cho, Y. M.; Wu, W.-M.; Criddle, C. S. Fate of hexabromocyclododecane (HBCD), a common flame retardant, in polystyrene-degrading mealworms: Elevated HBCD levels in egested polymer but no bioaccumulation. *Environ. Sci. Technol.* **2020**, *54* (1), 364–371.
- (27) Lou, Y.; Li, Y.; Lu, B.; Liu, Q.; Yang, S. S.; Liu, B.; Ren, N.; Wu, W.-M.; Xing, D. Response of the yellow mealworm (*Tenebrio molitor*) gut microbiome to diet shifts during polystyrene and polyethylene biodegradation. *J. Hazard. Mater.* **2021**, *416*, No. 126222.
- (28) Peng, B.-Y.; Sun, Y.; Xiao, S.; Chen, J.; Zhou, X.; Wu, W.-M.; Zhang, Y. Influence of polymer size on polystyrene biodegradation in mealworms (*Tenebrio molitor*): Responses of depolymerization pattern, gut microbiome, and metabolome to polymers with low to ultrahigh molecular weight. *Environ. Sci. Technol.* **2022**, *56* (23), 17310–17320.
- (29) Peng, B.-Y.; Su, Y.; Chen, Z.; Chen, J.; Zhou, X.; Benbow, M. E.; Criddle, C.; Wu, W.-M.; Zhang, Y. Biodegradation of polystyrene by dark (*Tenebrio obscurus*) and yellow (*Tenebrio molitor*) mealworms (Coleoptera: Tenebrionidae). *Environ. Sci. Technol.* **2019**, *53* (9), S256–S265.
- (30) Peng, B.-Y.; Chen, Z.; Chen, J.; Zhou, X.; Wu, W.-M.; Zhang, Y. Biodegradation of polylactic acid by yellow mealworms (larvae of *Tenebrio molitor*) via resource recovery: A sustainable approach for waste management. *J. Hazard. Mater.* **2021**, *416*, No. 125803.
- (31) Peng, B.-Y.; Chen, Z.; Chen, J.; Yu, H.; Zhou, X.; Criddle, C. S.; Wu, W.-M.; Zhang, Y. Biodegradation of polyvinyl chloride (PVC) in *Tenebrio molitor* (Coleoptera: Tenebrionidae) larvae. *Environ. Int.* **2020**, *145*, No. 106106.
- (32) Tsochatzis, E. D.; Berggreen, I. E.; Norgaard, J. V.; Theodoridis, G.; Dalsgaard, T. K. Biodegradation of expanded polystyrene by mealworm larvae under different feeding strategies evaluated by metabolic profiling using GC-TOF-MS. *Chemosphere* **2021**, *281*, No. 130840.
- (33) Wu, W.-M.; Criddle, C. S. Characterization of biodegradation of plastics in insect larvae. *Method Enzymol.* **2021**, *648*, 95–120.
- (34) Yang, Y.; Yang, J.; Wu, W.-M.; Zhao, J.; Song, Y.; Gao, L.; Yang, R.; Jiang, L. Biodegradation and mineralization of polystyrene by plastic-eating mealworms: Part 1. chemical and physical characterization and isotopic tests. *Environ. Sci. Technol.* **2015**, *49* (20), 12080–12086.
- (35) Yang, S.-S.; Wu, W.-M.; Brandon, A. M.; Fan, H. Q.; Receveur, J. P.; Li, Y.; Wang, Z. Y.; Fan, R.; McClellan, R. L.; Gao, S. H.; et al. Ubiquity of polystyrene digestion and biodegradation within yellow mealworms, larvae of *Tenebrio molitor* Linnaeus (Coleoptera: Tenebrionidae). *Chemosphere* **2018**, *212*, 262–271.
- (36) Yang, S.-S.; Ding, M.-Q.; Zhang, Z.-R.; Ding, J.; Bai, S.-W.; Cao, G.-L.; Zhao, L.; Pang, J.-W.; Xing, D.-F.; Ren, N.-Q.; et al. Confirmation of biodegradation of low-density polyethylene in dark-versus yellow- mealworms (larvae of *Tenebrio obscurus* versus *Tenebrio molitor*) via gut microbe-independent depolymerization. *Sci. Total Environ.* **2021**, *789*, No. 147915.
- (37) Yang, S.-S.; Ding, M. Q.; Ren, X. R.; Zhang, Z. R.; Li, M. X.; Zhang, L. L.; Pang, J. W.; Chen, C. X.; Zhao, L.; Xing, D. F.; et al. Impacts of physical-chemical property of polyethylene (PE) on depolymerization and biodegradation in insects yellow mealworms (*Tenebrio molitor*) and dark mealworms (*Tenebrio obscurus*) with high purity microplastics. *Sci. Total Environ.* **2022**, *828*, No. 154458.
- (38) Yang, S.-S.; Ding, M. Q.; He, L.; Zhang, C. H.; Li, Q. X.; Xing, D. F.; Cao, G. L.; Zhao, L.; Ding, J.; Ren, N. Q.; et al. Biodegradation of polypropylene by yellow mealworms (*Tenebrio molitor*) and superworms (*Zophobas atratus*) via gut-microbe-dependent depolymerization. *Sci. Total Environ.* **2021**, *756*, No. 144087.
- (39) Yang, S.-S.; Chen, Y.-d.; Zhang, Y.; Zhou, H.-M.; Ji, X.-Y.; He, L.; Xing, D.-F.; Ren, N.-Q.; Ho, S.-H.; Wu, W.-M. A novel clean production approach to utilize crop waste residues as co-diet for mealworm (*Tenebrio molitor*) biomass production with biochar as byproduct for heavy metal removal. *Environ. Pollut.* **2019**, *252*, 1142–1153.
- (40) Yang, S.-S.; Brandon, A. M.; Andrew Flanagan, J. C.; Yang, J.; Ning, D.; Cai, S. Y.; Fan, H. Q.; Wang, Z. Y.; Ren, J.; Benbow, E.; et al. Biodegradation of polystyrene wastes in yellow mealworms (larvae of *Tenebrio molitor* Linnaeus): Factors affecting biodegradation rates and the ability of polystyrene-fed larvae to complete their life cycle. *Chemosphere* **2018**, *191*, 979–989.
- (41) Yang, L.; Gao, J.; Liu, Y.; Zhuang, G.; Peng, X.; Wu, W.-M.; Zhuang, X. Biodegradation of expanded polystyrene and low-density polyethylene foams in larvae of *Tenebrio molitor* Linnaeus (Coleoptera: Tenebrionidae): Broad versus limited extent depolymerization and microbe-dependence versus independence. *Chemosphere* **2021**, *262*, No. 127818.
- (42) Peng, B.-Y.; Xu, Y.; Sun, Y.; Xiao, S.; Sun, J.; Shen, Z.; Chen, J.; Zhou, X.; Zhang, Y. Biodegradation of polyethylene (PE) microplastics by mealworm larvae: Physiological responses, oxidative stress, and residual plastic particles. *J. Clean. Prod.* **2023**, *402*, No. 136831.
- (43) Liu, J.; Liu, J.; Xu, B.; Xu, A.; Cao, S.; Wei, R.; Zhou, J.; Jiang, M.; Dong, W. Biodegradation of polyether-polyurethane foam in yellow mealworms (*Tenebrio molitor*) and effects on the gut microbiome. *Chemosphere* **2022**, *304*, No. 135263.
- (44) He, L.; Yang, S.-S.; Ding, J.; He, Z.-L.; Pang, J.-W.; Xing, D.-F.; Zhao, L.; Zheng, H.-S.; Ren, N.-Q.; Wu, W.-M. Responses of gut microbiomes to commercial polyester polymer biodegradation in *Tenebrio molitor* Larvae. *J. Hazard. Mater.* **2023**, *457*, No. 131759.
- (45) Peng, B.-Y.; Sun, Y.; Zhang, X.; Sun, J.; Xu, Y.; Xiao, S.; Chen, J.; Zhou, X.; Zhang, Y. Unveiling the residual plastics and produced toxicity during biodegradation of polyethylene (PE), polystyrene (PS), and polyvinyl chloride (PVC) microplastics by mealworms (larvae of *Tenebrio molitor*). *J. Hazard. Mater.* **2023**, *452*, No. 131326.

- (46) Tsochatzis, E. D.; Berggreen, I. E.; Vidal, N. P.; Roman, L.; Gika, H.; Corredig, M. Cellular lipids and protein alteration during biodegradation of expanded polystyrene by mealworm larvae under different feeding conditions. *Chemosphere* **2022**, *300*, No. 134420.
- (47) Yang, Y.; Wang, J.; Xia, M. Biodegradation and mineralization of polystyrene by plastic-eating superworms *Zophobas atratus*. *Sci. Total Environ.* **2020**, *708*, No. 135233.
- (48) Liu, P.; Qian, L.; Wang, H.; Zhan, X.; Lu, K.; Gu, C.; Gao, S. New insights into the aging behavior of microplastics accelerated by advanced oxidation processes. *Environ. Sci. Technol.* **2019**, *53* (7), 3579–3588.
- (49) Ouyang, M. Y.; Liu, J. H.; Wen, B.; Huang, J. N.; Feng, X. S.; Gao, J. Z.; Chen, Z. Z. Ecological stoichiometric and stable isotopic responses to microplastics are modified by food conditions in koi carp. *J. Hazard. Mater.* **2021**, *404* (Pt A), No. 124121.
- (50) Knossow, N.; Siebner, H.; Bernstein, A. Isotope analysis method for the herbicide bromoxynil and its application to study photo-degradation processes. *J. Hazard. Mater.* **2020**, *388*, No. 122036.
- (51) Lou, Y.; Ekaterina, P.; Yang, S.-S.; Lu, B.; Liu, B.; Ren, N.; Corvini, P. F.-X.; Xing, D. Biodegradation of polyethylene and polystyrene by greater wax moth larvae (*Galleria mellonella* L.) and the effect of co-diet supplementation on the core gut microbiome. *Environ. Sci. Technol.* **2020**, *54* (5), 2821–2831.
- (52) Yue, W.; Yin, C. F.; Sun, L.; Zhang, J.; Xu, Y.; Zhou, N. Y. Biodegradation of bisphenol-A polycarbonate plastic by *Pseudoxanthomonas* sp. strain NyZ600. *J. Hazard. Mater.* **2021**, *416*, No. 125775.
- (53) Li, Q.; Zeng, A.; Jiang, X.; Gu, X. Are microplastics correlated to phthalates in facility agriculture soil? *J. Hazard. Mater.* **2021**, *412*, No. 125164.
- (54) Jiang, C.; Liu, S.; Zhang, T.; Liu, Q.; Alvarez, P. J. J.; Chen, W. Current methods and prospects for analysis and characterization of nanomaterials in the environment. *Environ. Sci. Technol.* **2022**, *56* (12), 7426–7447.
- (55) Hintersteiner, I.; Himmelsbach, M.; Buchberger, W. W. Characterization and quantitation of polyolefin microplastics in personal-care products using high-temperature gel-permeation chromatography. *Anal. Bioanal. Chem.* **2015**, *407* (4), 1253–1259.
- (56) Ivleva, N. P. Chemical analysis of microplastics and nanoplastics: Challenges, advanced methods, and perspectives. *Chem. Rev.* **2021**, *121* (19), 11886–11936.
- (57) Leslie, H. A.; van Velzen, M. J. M.; Brandsma, S. H.; Vethaak, A. D.; Garcia-Vallejo, J. J.; Lamoree, M. H. Discovery and quantification of plastic particle pollution in human blood. *Environ. Int.* **2022**, *163*, No. 107199.
- (58) Chamas, A.; Moon, H.; Zheng, J.; Qiu, Y.; Tabassum, T.; Jang, J. H.; Abu-Omar, M.; Scott, S. L.; Suh, S. Degradation rates of plastics in the environment. *ACS Sustain. Chem. Eng.* **2020**, *8* (9), 3494–3511.
- (59) Zhou, M.; Dunne, F. Mechanisms-based constitutive equations for the superplastic behaviour of a titanium alloy. *J. Strain Anal. Eng. Des.* **1996**, *31* (10), 187–196.
- (60) Cheong, B.; Lin, J.; Ball, A. Modelling of the hardening characteristics for superplastic materials. *J. Strain Anal. Eng. Des.* **2000**, *35* (3), 149–157.
- (61) Aleksandrov, S.; Goldstein, R. Kinetic equation for the grain size in processes of intense plastic deformation. *Doklady Physics* **2009**, *54* (12), 553–556.
- (62) Pischedda, A.; Tosin, M.; Degli-Innocenti, F. Biodegradation of plastics in soil: The effect of temperature. *Polym. Degrad. Stab.* **2019**, *170*, No. 109017.
- (63) Leejarkpai, T.; Suwanmanee, U.; Rudeekit, Y.; Mungcharoen, T. Biodegradable kinetics of plastics under controlled composting conditions. *Waste Manag.* **2011**, *31* (6), 1153–1161.
- (64) Baldera-Moreno, Y.; Pino, V.; Farres, A.; Banerjee, A.; Gordillo, F.; Andler, R. Biotechnological aspects and mathematical modeling of the biodegradation of plastics under controlled conditions. *Polymers (Basel)* **2022**, *14* (3), 375.
- (65) Liu, T.; Chen, J.; Li, N.; Xiao, S.; Huang, C. H.; Zhang, L.; Xu, Y.; Zhang, Y.; Zhou, X. Unexpected role of nitrite in promoting transformation of sulfonamide antibiotics by peracetic acid: Reactive nitrogen species contribution and harmful disinfection byproduct formation potential. *Environ. Sci. Technol.* **2022**, *56* (2), 1300–1309.
- (66) Li, N.; Liu, T.; Xiao, S.; Chen, J.; Xu, Y.; Ji, R.; Zhou, X.; Zhang, Y. Iron cycle tuned by thiosulfate in Fenton reactions: Kinetic modelling and mechanisms. *Chem. Eng. J.* **2022**, *431*, No. 134252.
- (67) Wang, L.; Peng, Y.; Xu, Y.; Zhang, J.; Liu, C.; Tang, X.; Lu, Y.; Sun, H. Earthworms' degradable Bioplastic diet of polylactic acid: Easy to break down and slow to excrete. *Environ. Sci. Technol.* **2022**, *56* (8), 5020–5028.
- (68) Liu, J.; Qin, J.; Zhu, L.; Zhu, K.; Liu, Z.; Jia, H.; Lichtfouse, E. The protective layer formed by soil particles on plastics decreases the toxicity of polystyrene microplastics to earthworms (*Eisenia fetida*). *Environ. Int.* **2022**, *162*, No. 107158.
- (69) Yang, S.-S.; Chen, Y.-d.; Kang, J.-H.; Xie, T.-R.; He, L.; Xing, D.-F.; Ren, N.-Q.; Ho, S.-H.; Wu, W.-M. Generation of high-efficient biochar for dye adsorption using frass of yellow mealworms (larvae of *Tenebrio molitor* Linnaeus) fed with wheat straw for insect biomass production. *J. Clean. Prod.* **2019**, *227*, 33–47.
- (70) Zhang, Z.; Peng, H.; Yang, D.; Zhang, G.; Zhang, J.; Ju, F. Polyvinyl chloride degradation by a bacterium isolated from the gut of insect larvae. *Nat. Commun.* **2022**, *13* (1), 5360.
- (71) Peng, B.-Y.; Li, Y.; Fan, R.; Chen, Z.; Chen, J.; Brandon, A. M.; Criddle, C. S.; Zhang, Y.; Wu, W.-M. Biodegradation of low-density polyethylene and polystyrene in superworms, larvae of *Zophobas atratus* (Coleoptera: Tenebrionidae): Broad and limited extent depolymerization. *Environ. Pollut.* **2020**, *266*, No. 115206.
- (72) Inderthal, H.; Tai, S. L.; Harrison, S. T. L. Non-hydrolyzable plastics—an interdisciplinary look at plastic bio-oxidation. *Trends Biotechnol.* **2021**, *39* (1), 12–23.
- (73) Zhu, D.; Chen, Q.-L.; An, X.-L.; Yang, X.-R.; Christie, P.; Ke, X.; Wu, L.-H.; Zhu, Y.-G. Exposure of soil collembolans to microplastics perturbs their gut microbiota and alters their isotopic composition. *Soil Biol. Biochem.* **2018**, *116*, 302–310.
- (74) Kim, H. R.; Lee, H. M.; Yu, H. C.; Jeon, E.; Lee, S.; Li, J.; Kim, D. H. Biodegradation of polystyrene by *Pseudomonas* sp. isolated from the gut of superworms (larvae of *Zophobas atratus*). *Environ. Sci. Technol.* **2020**, *54* (11), 6987–6996.
- (75) Napper, I. E.; Thompson, R. C. Environmental deterioration of biodegradable, oxo-biodegradable, compostable, and conventional plastic carrier bags in the sea, soil, and open-air over a 3-year period. *Environ. Sci. Technol.* **2019**, *53* (9), 4775–4783.
- (76) Napper, I. E.; Bakir, A.; Rowland, S. J.; Thompson, R. C. Characterisation, quantity and sorptive properties of microplastics extracted from cosmetics. *Mar. Pollut. Bull.* **2015**, *99* (1–2), 178–185.
- (77) Wang, S.; Shi, W.; Huang, Z.; Zhou, N.; Xie, Y.; Tang, Y.; Hu, F.; Liu, G.; Zheng, H. Complete digestion/biodegradation of polystyrene microplastics by greater wax moth (*Galleria mellonella*) larvae: Direct *in vivo* evidence, gut microbiota independence, and potential metabolic pathways. *J. Hazard. Mater.* **2022**, *423* (B), No. 127213.
- (78) Woo, S.; Song, I.; Cha, H. J. Fast and facile biodegradation of polystyrene by the gut microbial flora of *Plesiophthalmus davidi* larvae. *Appl. Environ. Microbiol.* **2020**, *86* (18), No. e01361-20.
- (79) Kundugal, H.; Synshiang, K.; Devipriya, S. P. Biodegradation of polystyrene wastes by a newly reported honey bee pest *Uloma* sp. larvae: An insight to the ability of polystyrene-fed larvae to complete its life cycle. *Environ. Chall.* **2021**, *4*, No. 100083.
- (80) Kundugal, H.; Gangarapu, M.; Sarangapani, S.; Patchaiyappan, A.; Devipriya, S. P. Efficient biodegradation of polyethylene (HDPE) waste by the plastic-eating lesser waxworm (*Achroia grisella*). *Environ. Sci. Poll. Resear.* **2019**, *26*, 18509–18519.
- (81) Sanluis-Verdes, A.; Colomer-Vidal, P.; Rodriguez-Ventura, F.; Bello-Villarino, M.; Spinola-Amilibia, M.; Ruiz-Lopez, E.; Illanes-Vicioso, R.; Castroviejo, P.; Aiese Cigliano, R.; Montoya, M.; et al. Wax worm saliva and the enzymes therein are the key to polyethylene degradation by *Galleria mellonella*. *Nat. Commun.* **2022**, *13* (1), 5568.

- (82) Bombelli, P.; Howe, C. J.; Bertocchini, F. Polyethylene bio-degradation by caterpillars of the wax moth *Galleria mellonella*. *Curr. Biol.* **2017**, *27* (8), R292–R293.